Photocatalytic reduction of hexavalent chromium (Cr(VI)) using rotating TiO$_2$ mesh

Jaekyung Yoon, Eunjung Shim, and Hyunku Joo[†]

New and Renewable Energy Research Division, Korea Institute of Energy Research,
71-2 Jang-dong, Yuseong-gu, Daejeon 305-343, Korea

Abstract−An immobilized TiO$_2$ electrode for photocatalytic hydrogen production is applied to reduce toxic Cr(VI) to non toxic Cr(III) in aqueous solution under UV irradiation. To overcome the limitation of powder TiO$_2$, a novel technique of immobilization based on anodization was applied and investigated under various experimental conditions. The anodization was performed with three different electrolytes (single or mixed), and then the anodized samples were annealed under an oxygen stream. Among the three kinds of anodized/annealed TiO$_2$ on Ti foil, Sample II (anodized at 20 V in 0.5% HF for 45 min at 5 $^\circ$C, and annealed at 450 $^\circ$C for 5 hr in ambient oxygen at a flow rate of 400 mL/min) was more effective for both Cr(VI) reduction than the other samples. Based on the electrolyte compositions, nanotubular TiO$_2$ grown on Ti meshes was fabricated for the purpose of its light-harvesting ability and efficiency, where the anodized/annealed TiO$_2$ on meshes were rotated in the center of the reactor and Cr(VI) could be effectively reduced at rotation speeds ranging from 0 to 64 rpm. In case of Sample II, it was found that up to 98 % of the Cr(VI) was reduced in 30 min at 64 rpm.

Key words: Cr(VI) Reduction, Immobilized TiO$_2$, Anodization, Rotating Mesh Type Reactor

INTRODUCTION

Photocatalysis is an attractive technology for hydrogen production by water splitting and for environmental treatment. During the past several decades, many studies have attempted to improve the efficiency of hydrogen production and environmental remediation with photocatalysts. However, the photocatalytic process has been simultaneously criticized as being uneconomical compared to other systems, due to its inherently low efficiency, and the limitations of immobilization, which may increase the overall costs [1].

Conventional photocatalysis based on slurry type TiO$_2$ poses a problem of catalyst recovery after the reaction. Therefore, in this study, we focus on the reduction of toxic chromium (Cr(VI)) to non-toxic chromium (Cr(III)) with an immobilized TiO$_2$ photocatalyst under various conditions.

The band-gap energy of TiO$_2$ is 3.2 eV, which is equivalent to UV light with a wavelength of 380 nm, and TiO$_2$ is therefore photoexcited by near UV illumination. The holes that are generated on the TiO$_2$ are highly oxidizing, and there have been numerous studies on the utilization of TiO$_2$ in the oxidative degradation of organic contaminants by OH radicals (OH·). In addition, inorganic species with a reduction potential more positive than that of the conduction band of a semiconductor can consume the electrons and complete the redox reaction cycle. Recently, increasing attention has been paid to the photocatalytic reduction of inorganic contaminants. The TiO$_2$ photocatalytic reduction process has been reported to be effective for the removal of various toxic metal ions, such as Hg(II) [2], As(V)/As(III) [3,4], and Cr(VI) [5-9]. Besides TiO$_2$, the use of ZnO [10] and CdS [11] in the photocatalytic reduction of Cr(VI) to Cr(III) has also been reported.

Chromium occurs in two common oxidation states in nature, Cr(III) and Cr(VI). Cr(VI) is toxic to most organisms, carcinogenic in animals, and causes irritation and corrosion of the skin in humans. It is highly soluble in water and forms the mono- and divalent oxyanions, chromate (HCrO$_4^-$/CrO$_4^{2-}$) and dichromate (Cr$_2$O$_7^{2-}$), respectively, depending on its concentration and the pH of the solution. Because it is only weakly sorbed onto inorganic surfaces, Cr(VI) is mobile in nature. On the other hand, Cr(III) is readily precipitated or sorbed on a variety of inorganic and organic substrates at neutral or alkaline pH. Therefore, the reduction of Cr(VI) to Cr(III) is highly desirable in order to reduce its toxicity. After the reduction of Cr(VI), the resultant Cr(III) can be separated by several procedures, and then precipitated in neutral or alkaline solution in the form of Cr(OH)$_3$ [12-15].

In our previous study, we assessed the feasibility of using immobilized nanotubular TiO$_2$ grown on pure Ti foil for environmental remediation as well as hydrogen production [16,21-23]. The major conclusions of this preliminary study were as follows. First, the photocatalytic Cr(VI) reduction efficiency increased with decreasing pH value. In this study, the Cr(VI) reduction efficiency was about 98% under acidic conditions (pH 3) with anodized nanotubular TiO$_2$ annealed at 450 $^\circ$C. In addition, the results of the zeta potential and XRD measurements explained the surface characteristics and the reactivity with Cr(VI); the zeta potential became more positive with decreasing pH (pH 3) and stronger electrostatic affinity with the negatively charged Cr(VI) in water. By comparing the XRD patterns, it was shown that the anodized TiO$_2$ annealed at relatively lower temperature (450-650 $^\circ$C) had higher reduction efficiencies.

Based on these preliminary results, the purpose of the present work is to grow nanotubular TiO$_2$ on Ti substrates (foil and mesh) with various anodizing electrolytes, evaluate their Cr(VI) reduction

[†]To whom correspondence should be addressed.
E-mail: hkjoo@kier.re.kr

efficiency, and improve the reactor configuration in order to increase the Cr(VI) reduction efficiency by using rotating TiO$_2$ grown on Ti mesh. In our previous work, Cr(VI) reduction was performed on anodized TiO$_2$ grown on Ti foil. However, here, we used anodized TiO$_2$ on Ti mesh for the purpose of Cr(VI) reduction. The advantages of using a mesh type catalyst are that it is easy to attach and detach the number of anodized TiO$_2$ (meshes) to the rotating shaft in the middle of the reactor, and regulate the rotating speed of the mesh in order to increase the Cr(VI) reduction efficiency.

EXPERIMENTAL

1. Apparatus and Analysis

The experiments were conducted in a photocatalytic reactor with a volume of 200 ml that contained an aqueous solution whose initial concentration of Cr(VI) and pH varied. The outside of the reactor was water-jacketed to keep the reaction temperature constant. Prior to the reaction, the immobilized nanotubular TiO$_2$ on the meshes were rotated in the middle of the aqueous solution under the irradiation of UV light. Four of the nanotubular TiO$_2$ meshes were attached vertically to the central shaft of the bar rotator. The meshes were then placed vertically in the reactor and rotated at 24-64 rpm by means of motor, as shown in Fig. 1.

The light source used was a 1,000 W xenon lamp (Oriel, USA), which was filtered through a 10-cm IR filter. The light emission was above the wavelength of 300 nm, and the irradiated light intensity was measured to be ca. 68 mW/cm^2 (300-400 nm) by using a portable radiometer (UM-360, MINOLTA, Japan). Furthermore, the light intensity absorbed by the TiO$_2$ seemed to be slightly lower than the irradiated intensity, due to loss by reflection and absorption by the window and water.

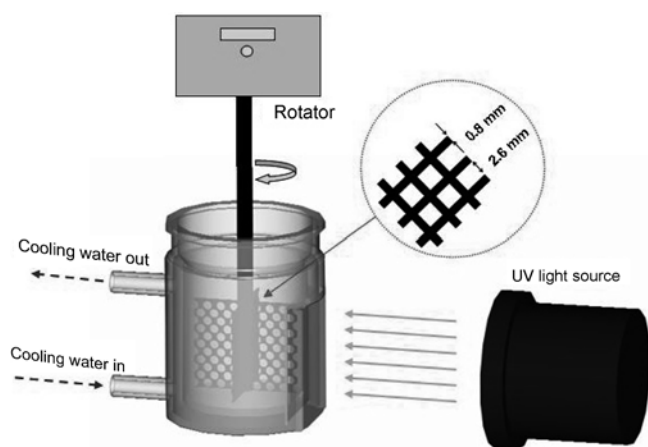The crystal phase and size were determined by X-ray diffraction (XRD, Miniflex, Rigaku, Japan; k=0.89, lambda=0.15418 for CuK X-ray, 30 kV, 15 mA) and the concentration of Cr(VI) was analyzed colormetrically by using UV/Vis spectroscopy (SCINCO, S-3150, Korea). In this analysis, the 1,5-diphenylcarbarzide method was used [17,18]. The structure and morphological characterizations were conducted by scanning election microscopy (SEM, Hitachi S-4700, Japan).

2. Preparation of Anodized Nanotubular TiO$_2$

All chemicals were used without further purification. Anodized nanotubular TiO$_2$ was used as a reference photocatalyst for measuring the reactivity in the reduction of Cr(VI). For the anodization experiments, titanium foils (0.25 mm thickness, Goodfellow, England) and meshes (1.2 mm thickness, Hyundai Titanium, Korea) were cut into pieces (2 cm×4 cm) and a two-electrode configuration was used. A coil-shaped platinum electrode served as the cathode. The anodization was performed at 20 V for 45 min with magnetic stirring, after which the samples were annealed under an oxygen stream (400 ml/min) at a temperature of 450 °C. The detailed conditions are summarized in Table 1. Three kinds of nanotubular TiO$_2$ arrays were formed by anodization of the Ti substrates in various electrolytes [19-21].

RESULTS AND DISCUSSION

A series of experiments were conducted with TiO$_2$ anodized at the same voltage (20 V) and different temperatures with various electrolytes: Sample I (0.14 M NaF+0.1 M NaNO$_3$+0.5 M H$_3$PO$_4$) anodized at 20 V and 20 °C for 45 min, Sample II (0.5% HF) anodized at 20 V and 5 °C for 45 min, and Sample III (0.31 M KF+0.33 M C$_6$H$_5$O$_2$Na$_3$+1.24 M NaHSO$_4$) anodized at 20 V and 20 °C for 45

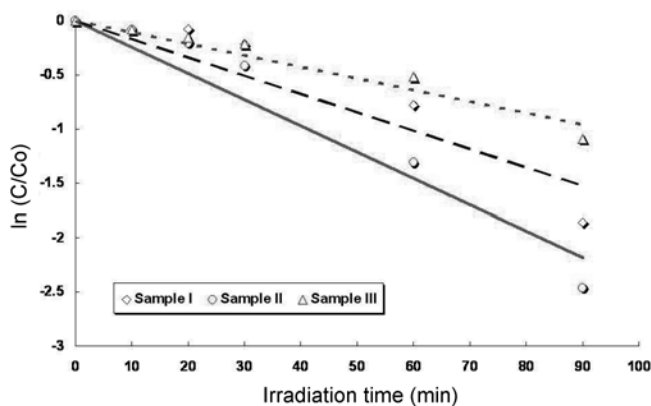Fig. 1. Schematic view of rotating mesh type photocatalytic reactor system.

Fig. 2. Logarithmic plot adopted to obtain the rate constant of Cr (VI) reduction for three anodized TiO$_2$ samples ([Cr(VI)$_o$ =38.5 μM, pH 3 adjusted with HNO$_3$, annealed at 450 °C for 5 hr in ambient oxygen at a flow rate of 400 mL/min, TiO$_2$ sample size (foil type): 1 cm^2).

Table 1. The fabrication conditions of the three TiO$_2$ samples used for Cr(VI) reduction

Sample	Electrolyte composition	Anodization	Annealing condition
Sample I	0.14 M NaF+0.1 M NaNO$_3$+0.5 M H$_3$PO$_4$	20 V at 20 °C for 45 min	450 °C for 5 hr in an oxygen
Sample II	0.5% HF	20 V at 5 °C for 45 min	atmosphere (400 ml/min)
Sample III	0.31 M KF+0.33 M C$_6$H$_5$O$_2$Na$_3$+1.24 M NaHSO$_4$	20 V at 20 °C for 45 min	

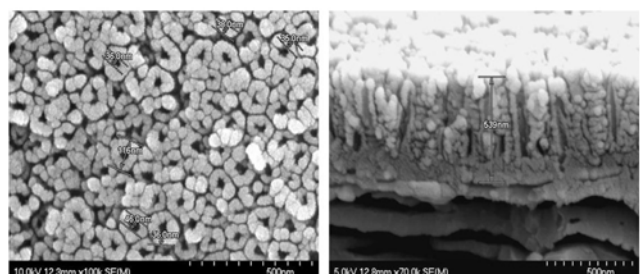**Table 2. Photocatalytic reduction efficiency and rate constant of Cr(VI) for three TiO₂ (foil type) samples**

Sample	% Cr(VI) reduction (90 min)	$k_{red} \times 10^2$ (min^{-1})
Sample I	84.4	1.69
Sample II	91.5	2.43
Sample III	63.4	1.07
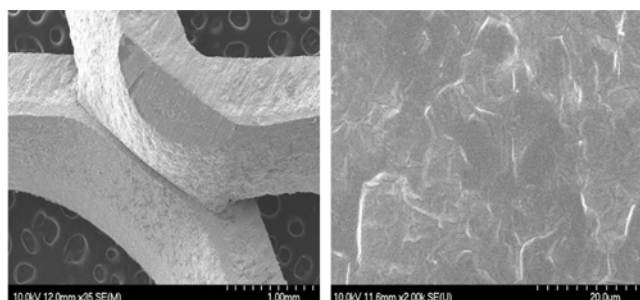
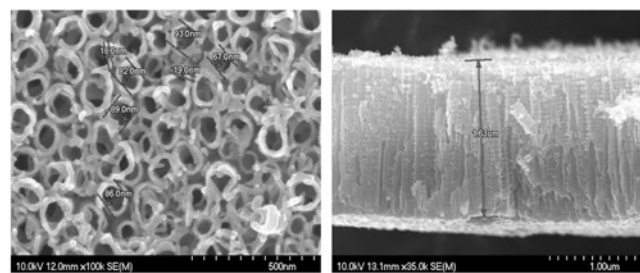
(a)
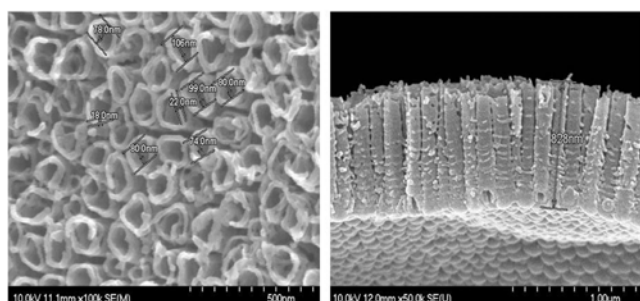
(b)

(c)


(d)

Fig. 3. SEM images of (a) Ti mesh (before anodization), (b) Sample I (anodized in 0.14 M NaF+0.1 M NaNO₃+0.5 M H₃PO₄ at 20 V-20 °C for 45 min), (c) Sample II (anodized in 0.5% HF at 20 V at 5 °C for 45 min), and (d) Sample III (anodized in 0.31 M KF+0.33 M C₆H₅O₂Na₃+1.24 M NaHSO₄ at 20 V at 20 °C for 45 min), and then commonly annealed at 450 °C for 5 hr in an oxygen atmosphere (400 ml/min).

min. After anodization, all three samples were annealed at 450 °C in ambient oxygen to provide an effective crystal structure of photocatalyst for Cr(VI) reduction [16].

Prior to the Cr(VI) reduction tests with rotating TiO₂ meshes conducted in this study [21-23], the three TiO₂ samples (foil type) were used as a photo-anode for hydrogen evolution tests in an enzymatic photo-electrochemical system (PEC). On the basis of the hydrogen evolution rate, sample II was found to show better hydrogen production (72.4 μmol/cm²-hr) than the other samples (66.2 μmol/cm²-hr for Sample I and 40.9 μmol/cm²-hr for Sample III). In addition, the rate constant (k) values of Cr(VI) reduction for the three TiO₂ samples (foil type), evaluated by linear fitting of the logarithmic plot in Fig. 2, are listed in Table 2 together with the Cr(VI) reduction efficiencies at a reaction time of 90 min. In these results, Sample II showed a higher hydrogen evolution rate, Cr(VI) reduction efficiency (91.5%), and rate constant (2.43 min^{-1}) than the other two samples.

Fig. 3 shows the SEM images of the anodized TiO₂ used in this study. As shown in Fig. 3(b) to (d), the tubes grow perpendicular to the substrate forming an array. The tubes on the three TiO₂ samples have lengths of 700-800 nm, 350-600 nm, and 1.5-1.6 μm, inner diameters of 80-100 nm, 40-60 nm, and 70-90 nm and wall thicknesses of 10-20 nm, 40-50 nm, and 15-20 nm, respectively. The morphological investigation showed that Sample II is different from that of the other samples, being denser and thicker. In addition, the tube length of Sample III is 2 times greater than those of the other two samples. In those cases where the same annealing temperature but different electrolyte compositions and anodization temperatures are used, the electrolyte composition at the different anodization temperature determines the morphological shape, with tube arrays being observed on the Ti mesh at an annealing temperature of 450 °C, as shown in Fig. 3(b) to (d) [24,25]. Also, as the annealing temperature is increased above 650 °C (not shown in Fig. 3), the Cr(VI) reduction efficiencies were significantly decreased and the tubular shape disappeared, with the result that a dense oxide film was found
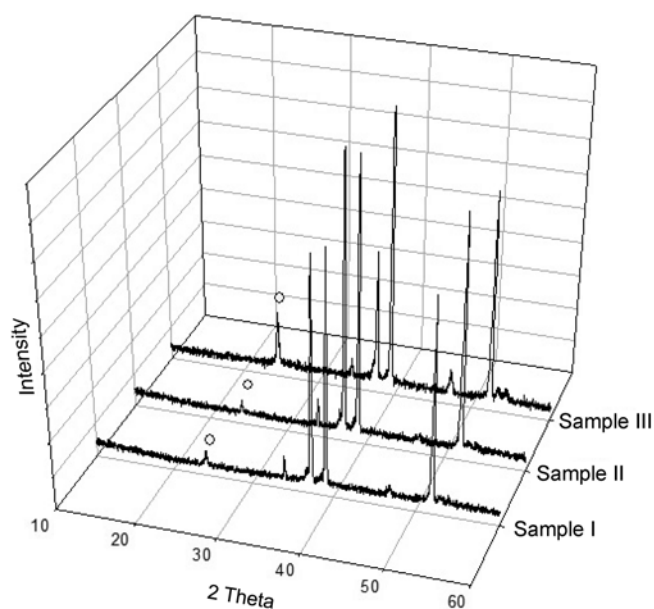
Fig. 4. XRD patterns of three TiO₂ samples (●: anatase phase).

on the Ti substrate [16].

The measured XRD spectra of the samples with the three kinds of electrolytes used for the photocatalytic Cr(VI) reduction are shown in Fig. 4. The TiO$_2$ that was only anodized but not annealed was amorphous and the anodized TiO$_2$ annealed at 450 °C consisted of anatase phase (circle). Several properties are known to affect the photocatalytic activity, such as the particle size, crystal structure, crystallinity and so on. Among these properties, it is well known that for the degradation of most pollutants, the anatase phase is the most active phase of TiO$_2$ [26]. In the comparison of the three samples, Sample III shows a larger peak for anatase phase than the other samples, because of the greater length of the tubular arrays on the

Ti substrate. However, Cr(VI) reduction with Sample III was lower than that obtained with the other samples, as shown in Fig. 2. With respect to their morphological properties, both Sample I and Sample III have a greater vertical length and smaller thickness than Sample II, which might be caused by the UV light not penetrating deeply into the nanotubular TiO$_2$.

Cr(VI) reduction was performed using three rotating TiO$_2$ meshes anodized with different electrolytes and the results are shown in Fig. 5. Four meshes, each anodized/annealed under one of the three different conditions and attached to the central shaft of the bar rotator, were rotated at speeds ranging from 24 to 64 rpm. In Fig. 5(a) to (c), the extent of Cr(VI) reduction increased with increasing rotation speed. At 64 rpm, up to 95% of the Cr(VI) was reduced in 90 min for all three samples. However, Sample II showed higher reduction efficiency than the other two samples. These results showed that in the case of Sample II, the highest reduction efficiency was obtained when the meshes were rotated at 64 rpm.

The effect of the initial concentration of Cr(VI) on the reduction efficiency was investigated by using four rotating meshes (Sample II) at a rotation speed of 64 rpm with different concentrations of Cr(VI) ranging from 38.5 to 154 μM (Fig. 6). As expected, the extent of reduction of Cr(VI) was less than 90% and 45% at initial concentrations of 77 and 154 μM, respectively, in these experiments, because of the small amount of TiO$_2$ on the Ti mesh. In other words, the dosage was insufficient to obtain a higher reduction efficiency of Cr(VI). In this study, the photocatalyst was immobilized TiO$_2$ anodized/annealed on Ti mesh, which was not a powder type catalyst such as commercial P25. Therefore, the dosage of TiO$_2$ grown on the Ti meshes introduced into the reactor was not determined, but an approximation is possible based on the general properties of the photocatalyst. Most of the tests in this study were performed with a TiO$_2$ mesh size of 8 cm^2 (2 cm×4 cm, porosity 20%), where the size can be directly related to the dosage, if the density of the photocatalyst is known. Assuming that the photocatalyst density is 3.9 g/cm^{-3} based on the results of a previous study [27] and the thickness of the anodized TiO$_2$ on the Ti mesh is ~600 nm (e.g., for Sample II) based on the SEM observation (Fig. 3), the quantity of anodized TiO$_2$ on the Ti mesh could be approximated to ~1.5 mg for a size of 8 cm^2 and, therefore, the quantity of anodized TiO$_2$ on the
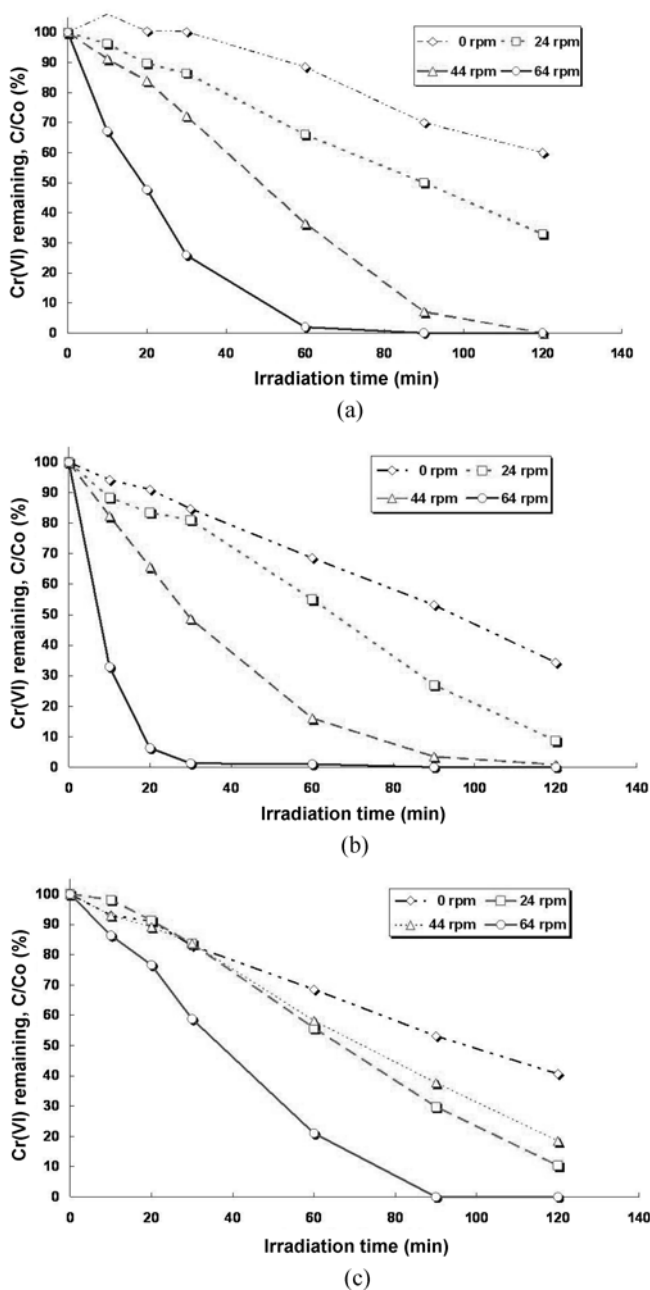

Fig. 5. Effect of rotating speed in the range of 0 to 64 rpm on Cr (VI) reduction with: (a) Sample I, (b) Sample II, and (c) Sample III ([Cr(VI)]$_o$=38.5 μM, pH 3 adjusted with HNO$_3$).
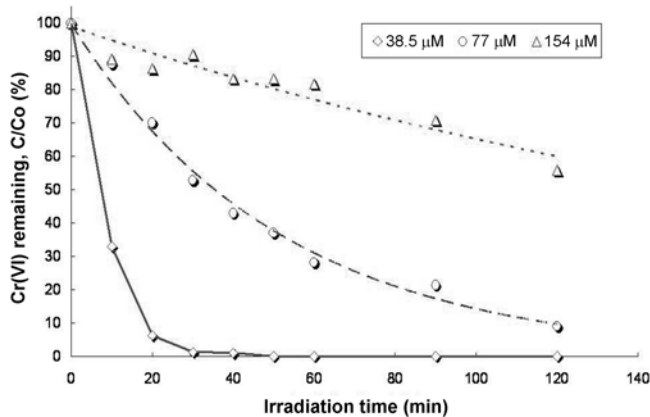

Fig. 6. Comparison of Cr(VI) reduction at different initial concentrations with Sample II (rotating speed at 64 rpm, pH 3 adjusted with HNO$_3$).

four Ti meshes was about 6.0 mg.

CONCLUSIONS

The aim of this work was to assess the feasibility of using immobilized TiO_2 for environmental remediation. The anodized nanotubular TiO_2 on Ti foil at the center of the reactor was shown to reduce 98% of Cr(VI) reduction in a 120 min. However, the purpose of present work was to improve the reactor configuration in order to increase the efficiency of Cr(VI) reduction by investigating various anodizing conditions and Ti materials from fixed type (foil) to rotated type (mesh) in the photocatalytic reactor.

Among the three TiO_2 samples (foil type), Sample II (anodized in 0.5% HF for 45 min at 5 °C) was more effective for photocatalytic hydrogen evolution and Cr(VI) reduction than Sample I (anodized in 0.14 M NaF+0.1 M $NaNO_3$+0.5 M H_3PO_4 for 45 min at 20 °C) and Sample III (anodized in 0.31 M KF+0.33 M $C_6H_5O_2Na_3$+1.24 M $NaHSO_4$ for 45 min at 20 °C). Based on the results obtained with the foil type TiO_2, four sorts of mesh type TiO_2 were fabricated for each anodizing/annealing condition and attached to the central shaft of the bar rotator. The results of the Cr(VI) reduction tests with the anodized/annealed meshes showed that, Sample II was more effective than the other samples as like those with foil type. In the case of Cr(VI) reduction with all of the samples, as the rotating speed of the meshes increased, the Cr(VI) reduction reaction became faster, with up to 95% of the Cr(VI) being reduced in 90 min. Especially, in the case of Sample II, the Cr(VI) was completely reduced in 30 min at a rotating speed of 64 rpm.

The XRD and SEM results explained the surface characteristics and the reactivity with Cr(VI). By comparing the XRD patterns, it was shown that Sample III having the anatase phase (450 °C) showed a larger anatase peak than the other samples, because of the greater length of the tubular arrays on the Ti meshes. However, samples having a greater vertical length and smaller thickness than those of Sample II might not make effective use of the UV light, because of the latter's not penetrating deeply into the nanotubular TiO_2. Finally, the SEM images supported the conclusion that the TiO_2 grown tubes were much more effective for Cr(VI) reduction.

ACKNOWLEDGMENTS

REFERENCES

1. M. Ashokkumar, *Int. J. Hydrogen Energy*, **23**, 427 (1998).
2. D. Chen and A. K. Ray, *Chem. Eng. Sci.*, **56**, 1561 (2001).
3. H. Yang, W. Y. Lin and K. Rajeshwar, *J. Photochem. Photobiol. A.*, **123**, 137 (1999).
4. H. Lee and W. Choi, *Environ. Sci. Technol.*, **36**, 3872 (2002).
5. Y. Ku and I.-L. Jung, *Wat. Res.*, **35**, 135 (2001).
6. J. J. Testa, M. A. Greala and M. I. Litter, *Langmuir*, **17**, 3515 (2001).
7. S. Rengaraj, S. Venkataraj, J. W. Yeon, Y. Kim, X. Z. Li and G. K. H. Pang, *Appl. Catal. B.*, **77**, 157 (2007).
8. X. R. Xu, H. B. Li and J. D. Gu, *Chemosphere*, **63**, 254 (2006).
9. P. Mohapatra, S. K. Samantray and K. Parida, *J. Photochem. Photobiol. A.*, **170**, 189 (2005).
10. L. B. Khalil, W. E. Mourad and M. W. Rophael, *Appl. Catal. B.*, **17**, 267 (1998).
11. S. Wang, Z. Wang and Q. Zhuang, *Appl. Catal. B.*, **1**, 257 (1992).
12. M. Costa, *Toxicol. Appl. Pharmacol.*, **188**, 1 (2003).
13. J. Yoon, G. Amy and Y. Yoon, *Wat. Sci. Technol.*, **51**, 327 (2005).
14. S. Lawniczak, P. Lecomte and J. Ehrhardt, *Environ. Sci. Technol.*, **35**, 1350 (2001).
15. M. A. Schlautman and I. Han, *Wat. Res.*, **35**, 1534 (2001).
16. J. Yoon, E. Shim, S. Bae and H. Joo, *J. Hazard. Mater.*, in press (2008).
17. V. Osokov, B. Kebbekus and D. Chesbro, *Anal. Lett.*, **29**, 1829 (1996).
18. X. Wang, S. O. Pehkonen and A. K. Ray, *Ind. Eng. Chem. Res.*, **43**, 1665 (2004).
19. G. K. Mor, K. Shankar, M. Paulose, O. K. Varghese and C. A. Grimes, *Nano Lett.*, **5**, 191 (2005).
20. G. K. Mor, K. Shankar, M. Paulose, O. K. Varghese and C. A. Grimes, *Sol. Enrg. Materls. & Sol. Cells*, **90**, 2011 (2006).
21. S. Bae, E. Shim, J. Yoon and H. Joo, *Sol. Enrg. Materls. & Sol. Cells*, **92**, 402 (2008).
22. S. Bae, J. Kang, E. Shim, J. Yoon and H. Joo, *J. Power Source*, **179**, 863 (2008).
23. S. Bae, E. Shim, J. Yoon and H. Joo, *J. Power Source*, **185**, 439 (2008).
24. D. Gong, C. A. Grimes, O. K. Varghese, W. Hu, R. S. Singh, Z. Chen and E. C. Dickey, *J. Mater. Res.*, **16**, 3331 (2001).
25. M. Paulose, G. K. Mor, O. K. Varghese, K. Shankar and C. A. Grimes, *J. Photochem. Photobiol. A: Chem.*, **178**, 8 (2006).
26. H. Jessen, K. D. Joensen, J.-E. Jorgensen, J. S. Pedersen and E. G. Sogaard, *J. Nanoparticle Res.*, **6**, 519 (2004).
27. N. Negishi, K. Takeuchi, T. Ibusuki and A. K. Dayte, *J. Mater. Sci. Lett.*, **18**, 515 (1999).